

## Determination of the vacancy migration enthalpy by Monte Carlo simulation of the short-range order kinetics by a vacancy diffusion mechanism in Ni-Al alloys.

Y.BELKADI <sup>a</sup>, M.Benkaddour <sup>b</sup>, J. Barkani <sup>c</sup>, D.Bahia <sup>b</sup>, A. Benkaddour <sup>a</sup>, S. Ramdani <sup>a</sup>

<sup>a</sup> Laboratory of Electromagnetic, Signal Processing & Renewable Energy (LESPRE), Team Electronic Materials & Renewable Energy (EMRE), Faculty of Science, Department of Physics Mohamed First University, Oujda, Morocco.

<sup>b</sup> Laboratory: Observatoire de la Lagune Marchica de Nador et Régions Limitrophes (OLMAN-RL), Multidisciplinary Faculty of Nador, University of Mohammed Premier Oujda, Morocco.

<sup>c</sup> Laboratory of Engineering Sciences (LSI), Polydisciplinary Faculty of Taza, University Sidi Mohamed Ben Abdellah, Fez.

### Abstract

Nickel-based superalloys are used for the manufacture of pieces evolving in hot parts of aircraft engines. They are constituted of a Ni<sub>3</sub>-Al long-range ordered intermetallic phase dispersed in a short-range order matrix corresponding to a nickel-based solid solution [1]. These materials have the particularity of having a high melting temperature, a relatively low density, a good resistance to oxidation and an extreme hardness [2]. Their performance strongly depends on the structural and dimensional stability (creep). They are therefore conditioned by atomic mobility and the properties of the vacancies. We proposed to study, a series of Nickel based alloys, presenting a short-range order and constituting the matrix' basis of these superalloys. In this work, the isothermal curves of electrical resistivity corresponding to ordering kinetics in a series of Ni-Al alloys, by the Monte Carlo method, were calculated up to the fourth neighbors. We have determined the migration enthalpies of the vacancy in these so-called alloys by the method of slope change [3].

\* Corresponding author:

[youssef.belkadi2@gmail.com](mailto:youssef.belkadi2@gmail.com)

Received 20 May 2019,

Revised 26 May 2019,

Accepted 26 May 2019

**Keywords:** Superalloys; Vacancy defect; Atomic order; Atomic mobility; Monte Carlo Simulation; Electrical resistivity.

## 1. Introduction

The Al-Ni alloys reveal outstanding mechanical and thermal properties including their ability to withstand extreme temperatures, corrosion, oxidation, and wear [4, 5]. A number of their characteristics, in particular, their microstructural stability and creep resistance, are directly related to matter transport and are therefore conditioned by the properties of the vacancy defects. The Ni-Al alloys studied in this work present a local phenomenon that has been developed by X-ray scattering [6, 7]. A thorough understanding of the thermal vacancy properties (formation energy and migration energy) will allow proper understanding and modeling of this phenomenon. Experimental studies carried out on Ni-Al alloys containing 6 and 10 % of Al [8, 9] have shown a strong positive correlation between the degree of order and the electrical resistance. In the present work, we have calculated the excess resistivity curves due to the formation of the local order at two temperatures:  $T_1 = 700K$  and  $T_2 = 900K$ . The vacancy migration enthalpy was determined by the method of the slope change used in experimental studies, developed by J.Barkani and al [3].

## 2. Method for determining the migration enthalpy of the vacancies.

The method we used to determine the vacancy migration enthalpy is to evaluate the electrical resistivity's change rate as a function of time,  $\dot{\rho}_n$  ( $n = 1, 2$ ) at the instant at which the order kinetic temperature  $T_n$  is changed. The relationship that allows the calculation of enthalpies of migration of the vacancy by this method is given by Schulze and Lücke [10]. It considers the contribution of order variations to electrical resistivity:

$$\Delta H_V^M = \frac{k}{\frac{1}{T_1} - \frac{1}{T_2}} \left[ \text{Log} \left( \frac{\dot{\rho}_2^A}{\dot{\rho}_1^A} \right) + \beta \text{Log} \left( \frac{\Delta \rho_1^A}{\Delta \rho_2^A} \right) \right]$$

$\dot{\rho}_1^A$  and  $\dot{\rho}_2^A$  being the speeds of variation of the electrical resistivity at a point A being far from the state of thermodynamic equilibrium at temperatures  $T_1$  and  $T_2$ ,  $\Delta \rho_1^A$  and  $\Delta \rho_2^A$  represent the difference between the resistivity at point A and the characteristic resistivity of the equilibrium order state at temperatures  $T_1$  and  $T_2$  and  $\beta$  is the exponent of the expression which relates the speed  $\dot{\rho}$  of variation of resistivity due to changes in the state of order and the difference  $(\rho_{eq} - \rho)$  to the order that must exist at the thermodynamic equilibrium  $(\rho_{eq})$ , that is [10, 11] :

$$\frac{\dot{\rho}}{\rho_{\infty}} = \frac{\vartheta}{m} \times \frac{C_V}{B^{\beta-1}} \times \left( \frac{\rho_{eq} - \rho}{\rho_{\infty}} \right)^{\beta}$$

With:  $B$  : Constant, suitably chosen,  $C_V$  : Concentration of the vacancies,  $\vartheta$  : Frequency of jumps of the vacancies,  $m$  : Average number of jumps of each atom, up to equilibrium and  $\rho_{\infty}$  : Electrical resistivity of the completely disordered state.

The principle of the simulation consists in a first phase to calculate the isotherms of the excess of resistivity due to the order,  $\left( \frac{\rho_1 - \rho_{\infty}}{\rho_{\infty}} \right)$  and  $\left( \frac{\rho_2 - \rho_{\infty}}{\rho_{\infty}} \right)$  as a function of time, at the respective temperatures  $T_1$  and  $T_2$ . From these curves, we determine  $\frac{\Delta \rho_1^A}{\rho_{\infty}}$  and  $\frac{\Delta \rho_2^A}{\rho_{\infty}}$  and therefore the ratio  $\frac{\Delta \rho_1^A}{\Delta \rho_2^A}$ . In a second phase, we determine from the isothermal curve  $\frac{\rho_1 - \rho_{\infty}}{\rho_{\infty}}$  at  $T_1$ , the value of the normalized electrical resistivity  $\frac{\rho_1^A(T_1) - \rho_{\infty}}{\rho_{\infty}}$  which characterizes the state of order at point A. We, then, project this corresponding value on the isotherm  $\frac{\rho_2 - \rho_{\infty}}{\rho_{\infty}}$  at  $T_2$  such that  $\rho_1^A(T_1) = \rho_2^A(T_2)$ . We, then, construct a graph, taking the part of the curve  $\frac{\rho_1 - \rho_{\infty}}{\rho_{\infty}}$  from the initial state to the point A and the part of the curve  $\frac{\rho_2 - \rho_{\infty}}{\rho_{\infty}}$  to beyond point A.

## 3. Results

### 3.1. Calculation model

Our study is carried out on Ni-Al binary alloys of face centered cubic structure, containing N sites. N was chosen to have a vacant site on a sample of length  $L = 64$  such that  $N = L^3$ . The concentration of the vacancies  $C_V^0$  considered in our calculations is therefore:

$$C_V^0 = \frac{1}{64^3} \cong 3,81 \times 10^{-6} \text{ lacunes}$$

The evolution of the state of order of the alloy, starting from a disordered reference state is followed by the calculation of the residual electrical resistivity, from the relation given by Rossiter and Wells [12]:

$$\frac{\Delta\rho_{OCD}}{\rho_\infty} = \frac{\rho - \rho_\infty}{\rho_\infty} = \sum_i Z_i \alpha_i Y_i$$

Where are  $\alpha_i$  the order parameters of Warren-Cowley. The  $Z_i$  are the coordination numbers and  $Y_i$  [12], functions that depend on the number of conduction electrons per atom.

It is noted that the evolution time of the system, starting from a disordered state, towards the state of order at thermodynamic equilibrium, depends on the actual concentration of the vacancies at the kinetic temperature considered. As a result, we have made corrections where necessary, and in particular we have corrected the rate of change of electrical resistivity  $\dot{\rho} = \frac{d\rho}{dt}$ , that we have noted  $\dot{\rho}_{corrigé}$ . Indeed, the time it takes to reach a defined configuration, having a value of the electrical resistivity characteristic of the order state, depends on the concentration of the vacancies. The time  $t_{MC}$  used in our calculations is proportional to the real time  $t_P$  [13, 14] and is given by:

$$t_P = t_{MC} \times \frac{C_V^0}{C_V^T}$$

Where  $C_V^T$  is the concentration of the vacancies at temperature  $T$ , that we have assumed equal to that of pure nickel and which is given by:

$$C_V^T = \exp\left(-\frac{\Delta S_V^F}{K_B}\right) \times \exp\left(-\frac{\Delta H_V^F}{K_B T}\right)$$

$$\text{With: } \exp\left(\frac{\Delta S_V^F}{K_B}\right) = 2.7 \text{ et } \Delta H_V^F = 1.8 \text{ eV}$$

### 3.2. Parameters used in our calculations.

The parameters we have used in our calculations, which are the cohesion energies, the interaction energies between atom pairs and atom-vacancy, the formation energies and vacancy migration, the pre-exponential factor of the diffusion and the frequency of attack are collected in table 1. The interaction energies of the pairs of atoms and the electronic structure parameters specific to each alloy are collated in Table 2.

**Table 1.** Parameters used in our calculations

Cohesion energy (eV)			Vacancy formation energy (eV)		
Ni	4.44	[17]	Ni	1.8	[1]
Al	3.36	[18]	Al	0.66	[15]
Vacancy migration energy (eV)			Self-diffusion enthalpy (eV)		
Ni	1.04	[16]	Ni	2.84	[1]
Al	0.65	[15]	Al	1.31	[19]
Pre-exponential factor (m <sup>2</sup> /s)			Frequency of attack (1/s)		
Ni	1.4x10 <sup>-4</sup>	[17]	$\nu_{Ni}$	1.13x 10 <sup>15</sup>	
Al	0.173x10 <sup>-4</sup>	[18]	$\nu_{Al}$	1.05x 10 <sup>14</sup>	

**Table 2.** Interaction energies of atom pairs and electronic structure parameters of Ni-Al alloys [1].

i(the number of neighbors)	1	2	3	4
$W_{Ni-Al}^i(ev)$	-0.138	0.017	0.006	0.025
$Y_i$	-0.085	-0.081	0.025	0.045

### 3.3. Curves of variation of the excess of normalized electrical resistivity due to ordering kinetics.

The curves of ordering isotherms of Ni-Al alloys obtained by the calculation of Monte Carlo simulation at the temperature  $T_1 = 700K$  and  $T_2 = 900K$ , going as far as interactions with the fourth neighbors, are presented in figures 1.a and 1.b. The excess resistivity due to ordering kinetics shows a rapid variation at the beginning of the kinetics and reaches the thermodynamic equilibrium saturation value for Monte Carlo times greater than  $1,8 \times 10^{31}$  at 700K and  $2 \times 10^{26}$  at 900K.

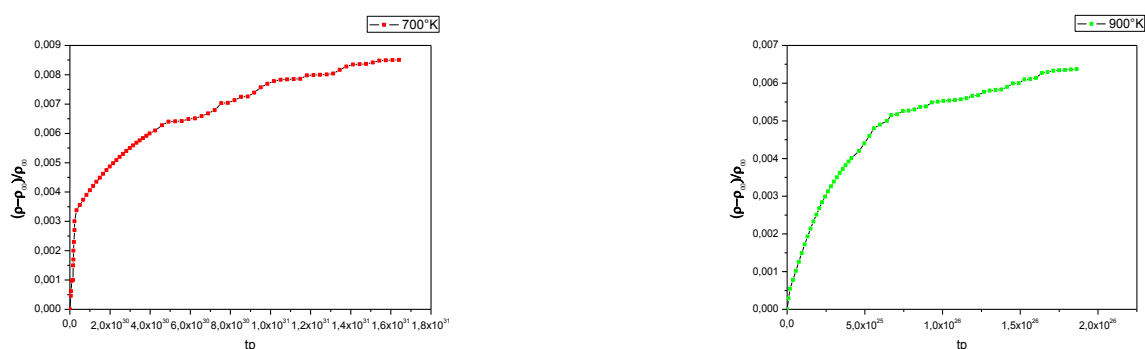


**Figure 1.a.** Variation of the electrical resistivity, due to the contribution of the local order in the alloy Ni-6at% Al as a function of time  $tp$  at 700 ° K and at 900K.

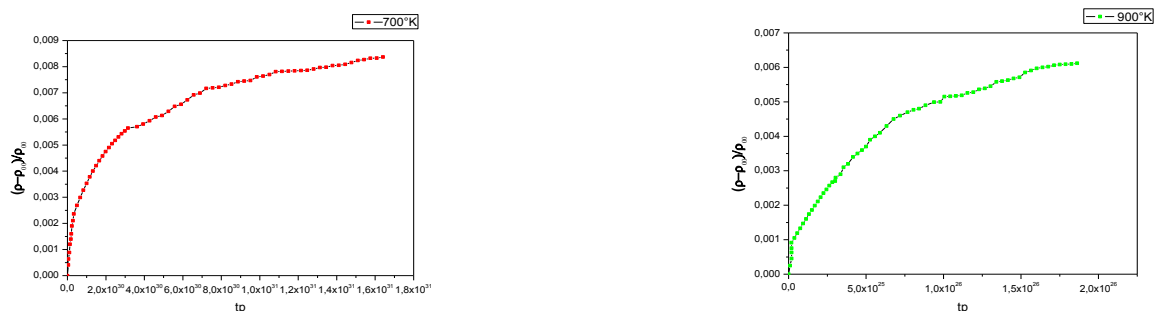


**Figure 1.b.** Variation of the electrical resistivity, due to the contribution of the local order in the alloy Ni-10at% Al as a function of time  $tp$  at 700 ° K and at 900K.

### 3.4. Enthalpy of vacancy migration in Ni-Al alloys

The vacancy migration enthalpy in the Ni-Al alloys studied was determined by the Schulze-Lücke relationship [9]. The deviations  $\frac{\Delta\rho_1^A}{\rho_\infty}$  and  $\frac{\Delta\rho_2^A}{\rho_\infty}$  are determined from the direct curves of variation of the excess of normalized resistivity as a function of time  $tp$ . The ratio of the resistivity variation speed  $\frac{\dot{\rho}_2^A}{\dot{\rho}_1^A}$  is determined from the derived curves  $\frac{\dot{\rho}_{corrected}}{\rho_\infty} = \frac{d\rho}{dt\,tp}$  (figures 2.a and 2.b) as a function of the normalized electrical resistivity difference at equilibrium. The coefficient  $\beta$  is determined from the curves (figures 3.a and 3.b) which are given by:

$$\text{Log}\left(\frac{\dot{\rho}}{\rho_\infty}\right) = f\left[\text{Log}\left(\left|\frac{\rho_{eq} - \rho}{\rho_\infty}\right|\right)\right]$$

The vacancy migration enthalpies and parameter values useful for their determinations are collected in Table 3.

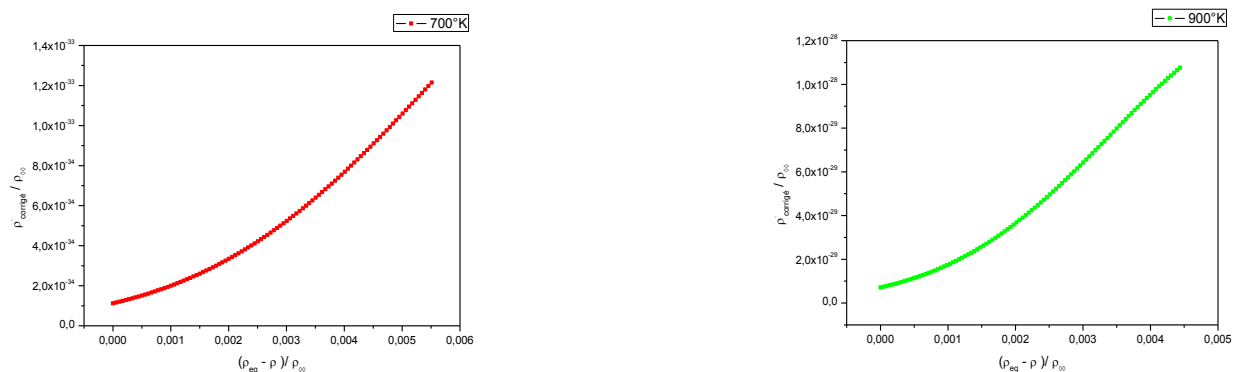


**Figure 2.a.** Rate of variation of the electrical resistivity of the Ni-6at% Al alloy, as a function of the difference in electrical resistivity normalized to the order of equilibrium at 700K and 900K.

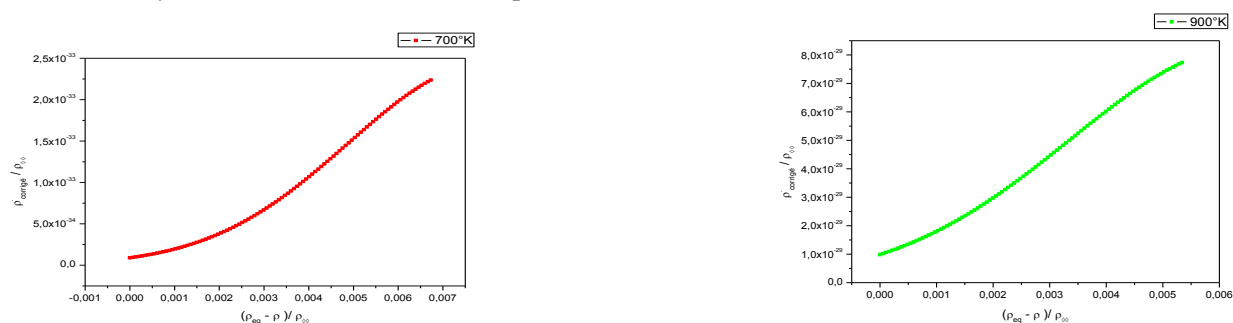


**Figure 2.b.** Rate of variation of the electrical resistivity of the Ni-10at% Al alloy, as a function of the difference in electrical resistivity normalized to the order of equilibrium at 700K and 900K.

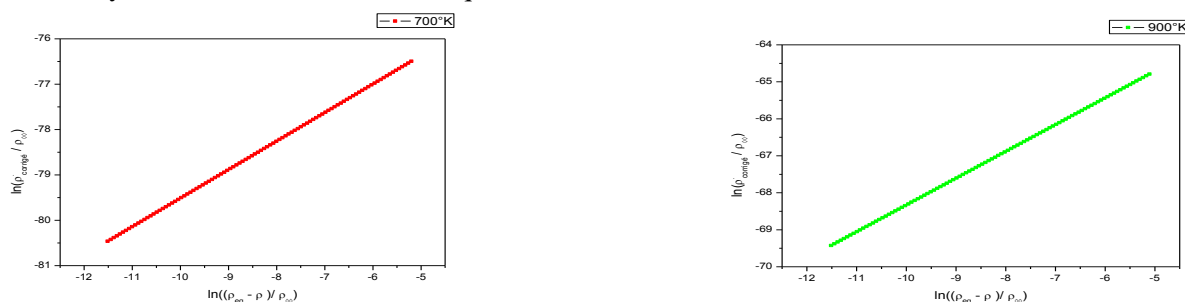


**Figure 3.a.** Logarithm of the rate of change of the electrical resistivity of the Ni-6at% Al alloy, as a function of the logarithm of the equilibrium difference at 700K and 900K.

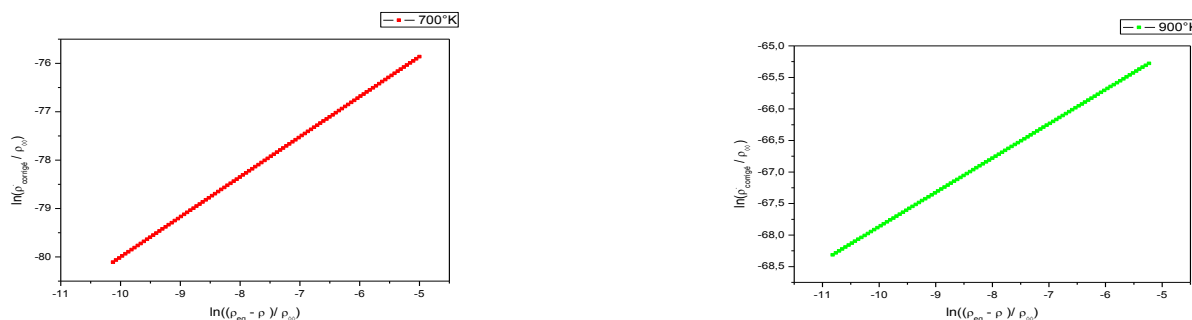


**Figure 3.b.** Logarithm of the rate of change of the electrical resistivity of the Ni-10at% Al alloy, as a function of the logarithm of the equilibrium difference at 700K and 900K.

**Table 3.** Values of the parameters appearing in the Schulze and Lücke relation and enthalpy of migration of the alloys Ni-6at% Al and Ni-10at% Al.

	$\frac{\Delta\rho_1^A}{\rho_\infty}$	$\frac{\Delta\rho_2^A}{\rho_\infty}$	$\frac{\dot{\rho}_1^A}{\rho_\infty}$	$\frac{\dot{\rho}_2^A}{\rho_\infty}$	$\beta$	$\Delta H_V^M$ (ev)
Ni-6at% Al	0,00353	0,00139	$3,05.10^{-34}$	$2,74.10^{-29}$	$0,67 \pm 0,08$	$1,51 \pm 0,01$
Ni-10at% Al	0,00347	0,00163	$3,31.10^{-34}$	$2,76.10^{-29}$	$0,68 \pm 0,09$	$1,46 \pm 0,01$

## 4. Conclusion

We have developed the "Monte Carlo" program for the simulation of vacancy mechanism ordering kinetics in Ni-6at% Al and Ni-10at% Al alloys. The migration enthalpies of the vacancy that we have determined in this work are higher than those in pure nickel. These differences are attributed to an effect of trapping vacancy by aluminum [8]. The migration enthalpy of the vacancies in the Ni-6at% Al alloy is greater than those in the Ni-10at% Al alloy. This difference is due to a ratio of the electrical resistivity variation rates  $\frac{\dot{\rho}_2^A}{\dot{\rho}_1^A}$  of the Ni-6at% Al alloy greater than those of the Ni-10at% Al alloy. Our values of vacancy migration enthalpies are slightly lower than those previously determined [20] but have a similar variation.

## References

- [1] Tarfa, T. thèse de doctorat de l'université paris VI, (1994).
- [2] Pope, D. P. and Darolia, R., in Applications of Intermetallic Compounds, MRS Bulletin (ed. JH Westbrook), (1996), 21 - 26.
- [3] Barkani, J. Benkaddour, A. Ramdani, S. Elhammouti, M. Roubi, L. Phys.Chem.News33(2007)72-79.
- [4] Chrifi-Alaoui, F.Z. Nassik, M. Kardellass, S. Azza, H. Selhaoui, N. J. Mater. Environ. Sci., (2018), Volume 9, Issue 4, Page 1098-1109.
- [5] Le Pévédic, S. Thèse de Doctorat de l'Université Pierre et Marie Curie - Paris VI, (2007).
- [6] Chassange F. Thèse Université Paris VI, (1986).
- [7] Klaiber F., Schönfeld B. et Kistorz G. Acta. Crystallogr. A(1987), 43-525.
- [8] Sitaud, B. thèse de doctorat de l'université paris 6, (1991).
- [9] Sitaud, B. Dimitrov, O. Journal of Physics: Condensed Matter, Volume 2, Number 34(1990)
- [10] Schulze, A. Lücke, K. Acta Metall., 20 (1972) 529.
- [11] Lücke K., Heidsiek, H. Khol, W. Scheffel, R. ed. JI Takamura et al (Tokyo: University of Tokyo press) (1982) p 647.
- [12] Rossiter, P.L. et Wells, phil, P.. Mag. 24 (1971) 425.
- [13] Soisson, F. Barbu, A. Martin, G. Acta Mater, 44 (1996) 3789.
- [14] Bouar, Y. L. Soisson, F. Phys. Rev. B, 65 (2002).
- [15] Aslanides, A. thèse de doctorat de l'université paris 6, (1998).
- [16] Dimitrov, O. Tarfa, T. Sitaud, B. Dimitrov, C. (1996), 06 (C2), pp.C2-79-C2-88
- [17] Kandaskalov, D. thèse de doctorat de l'université de Toulouse (2013).
- [18] Clouet, E. Nastar, M. Sigli, C. 69( 2004) 64109.
- [19] Engardt, R. D. and Barnes, R. G. American Physical Society, (1971).
- [20] Dimitrov, O. Tarfa, T. Sitaud, B. et Dimitrov, C. JOURNAL DE PHYSIQUE IV, Volume 6, mars (1996), C2-79.